Thermochemical Energy Storage with Integrated District Heat Production—A Case Study of Swede

(article starts on next page)

Thermochemical Energy Storage with Integrated District Heat Production—A Case Study of Sweden

Diana Carolina Guío-Pérez †, Guillermo Martinez Castilla *,†, David Pallarès, Henrik Thunman and Filip Johnsson

Division of Energy Technology, Chalmers University of Technology, 41296 Gothenburg, Sweden
* Correspondence: castilla@chalmers.se
† These authors contributed equally to this work.

Abstract: The implementation of electricity-charged thermochemical energy storage (TCES) using high-temperature solid cycles would benefit the energy system by enabling the absorption of variable renewable energy (VRE) and its conversion into dispatchable heat and power. Using a Swedish case study, this paper presents a process for TCES-integrated district heating (DH) production, assesses its technical suitability, and discusses some practical implications and additional implementation options. The mass and energy flows of a biomass plant retrofitted with an iron-based redox loop are calculated for nine specific scenarios that exemplify its operation under electricity generation mixes that differ with respect to variability and price. In addition, the use of two types of electrolyzers (low-temperature and high-temperature versions) is investigated. The results show that for the Swedish case, the proposed scheme is technically feasible and capable of covering the national DH demand by making use of the existing DH plants, with an estimated process energy efficiency (electricity to heat) of 90%. The results also show that for a retrofit of the entire Swedish DH fleet, the required inventories of iron are approximately 2.8 Mt for the intermediate scenario, which represents 0.3% and 11.0% of the national reserves and annual metallurgical production rates of the national industry, respectively. In addition to the dispatchable heat, the process generates a significant amount of nondispatchable heat, especially for the case that employs low-temperature electrolyzers. This added generation capacity allows the process to cover the heat demand while decreasing the maximum capacity of the charging side computed herein.

Keywords: variable renewable energy (VRE); thermochemical energy storage (TCES); iron looping; district heating (DH); electricity market; Nordic region

1. Introduction

It is well known that increasing the share of renewable energy sources in the electricity system is crucial for the decarbonization of such energy systems. In particular, variable renewable energy (VRE) in the form of wind and solar power generation has undergone strong growth in the past few decades and is expected to increase in the upcoming years [1–3]. However, given that VRE generation is inherently intermittent, as its share in a given energy system increases, so do the grid instabilities and the requirements for frequency and stability control. At the same time, systems with strong penetration of VRE experience periods of high availability and very low availability, or even negative electricity prices when the output from generation surpasses the demand. In fact, the misalignment of production and demand is the main reason for the curtailment of VRE generation and is therefore highly undesirable. Such misalignment can, to some extent, be reduced by implementing energy storage solutions. This, along with other variation management measurements, aims to achieve flexibility in the demand side (i.e., shifting the load in time to account for electricity price variations) [4,5].

The IEA [6] anticipates that energy storage, in general, will provide the flexibility and robustness needed to achieve a fully decarbonized energy system. Depending on the context, different variation management options (and combinations of options) for handling the variations in nondispatchable electricity generation on different time scales will be required [7,8]. The use of storage will enable VRE electricity to be harvested during the periods of highest availability and stored to be used during periods and at locations with a high level of demand and a low level of VRE production. Thus, energy storage can contribute to covering the net load curve (electricity demand minus VRE generation), and this will reduce the share of VRE that needs to be curtailed, thereby increasing the value of VRE. Storage can be in the form of pumped hydropower, batteries (both lithium based and vanadium flow), or hydrogen and other electrofuels. It can also take the form of heat by using the link between electricity and heat in district heating (DH) systems and electricity-based residential heating (using the thermal capacity of buildings as storage). Heat can be stored as latent or sensible heat. Different materials can be used for heat storage depending on the temperature of the source and that of the final application. However, the main drawback of thermal storage technologies is the heat losses that occur over time, which hinder seasonal storage. Note that because DH systems are based on the transmission of heat via a hot fluid (usually water), they have an inherent storage capacity, and some studies have quantified this storage capacity and evaluated its expansion. This can be achieved through the addition of hot water tanks, through the implementation of control tools, and in combination with storage to exploit the thermal capacities of buildings [9–11].

A promising technology that facilitates the storage of heat in the form of chemical energy is thermochemical energy storage (TCES). TCES offers the possibility to store energy for indefinite periods of time under ambient conditions. Many of the TCES systems achieve energy densities of the same order of magnitude as currently used fuels, making transport and storage economically attractive [12] and offering the possibility to discharge the heat at high temperatures (700–1000 °C). This enables the efficient conversion (if required) of the stored heat into electricity though conventional power cycles. Among the different materials considered for TCES, redox systems are often highlighted [13–15]. These systems are based on metal oxides for which the reduction step requires a significant amount of specific energy (per kg of reduced solid), which can be stored to be released later (and at a different location if so desired) in the oxidation step. Thus, TCES processes have the potential to absorb nondispatchable electricity and, thereafter, produce dispatchable DH and electricity. Such a scheme would increase the energy and resource efficiencies not only of regional energy systems (including the DH networks) but also of the national energy system (because the transportation of energy could be carried out without relying on the electricity transmission network) while boosting the penetration of VRE. The idea of combining TCES and DH is attractive because a large share of the available infrastructure of the DH system can be adapted to use a reduced metal as fuel [16,17]. DH plants based on solid fuels (fossil and nonfossil) in the Nordic countries typically use fluidized bed (FB) combustors (either bubbling or circulating), which can be retrofitted to process metal powders [18]. In addition, the water-steam equipment, as well as the hot water networks already in place, could remain unaltered.

Heating is an essential service that accounts for almost one-third of the final energy consumption in Europe. Therefore, it is important for energy security and decarbonization policies [19] and even more so following the Russian invasion of Ukraine [20,21]. In urban areas of the Nordic and Baltic countries, the heat demand is primarily met by DH systems that are powered by heat-only plants and combined heat and power (CHP) plants as well as through the use of waste heat from industrial processes. In Latvia, Estonia, Lithuania, Poland, Denmark, Sweden, and Finland, more than 50% of the inhabitants are supplied by DH [22], and the largest absolute consumption levels on a national basis are those of Poland, Germany, and Sweden (each of which surpassed 50 TWh in 2013), followed by Finland, Denmark, Czech Republic, Slovakia, France, and Austria (with national net

consumptions in the range of 20–40 TWh in 2013) [23]. In several of these countries, solid biomass (wood and municipal solid waste,MSW)–fired CHP units have been crucial in reducing the use of fossil fuels [24], as is the case in Sweden, Austria, and Estonia.

In this sense, given the significant share that heat demand has in the total energy consumption in a high percentage of European countries, there is growing interest in electricity-based heating systems that can be combined with storage, as a means to increase the penetration of VRE while dampening the variations in the electricity supply. Nevertheless, three aspects should be carefully considered. First, in a system with low flexibility, the direct electrification of heating systems would add a considerable load onto the electricity grid during periods when the electrical system is close to the limit of its capacity, and the electricity is produced at high cost. Second, using electricity for heating is obviously not desirable unless there is some additional benefit, such as the use of electricity during periods when there is an abundance of generated electricity, which would otherwise be curtailed. Third, the future distribution of the energy (both electricity and heat) demand will increase the stress on urban areas (forecasts indicate that more than 80% of European citizens will live in urban areas by 2050 [25]), meaning that electricity from VRE generation will need to be transmitted from regions of high availability to regions of high demand.

With regard to the electrification of the heating services, two technologies are highlighted in the literature as direct electrification options, namely electric boilers and heat pumps [26,27]. Electric boilers were commonly used in countries such as Sweden and Norway as single residential user solutions. However, they quickly became less attractive when taxes were imposed on electricity with the aim of reducing the dependency on electricity for heating (and to disincentivize exergetically inefficient uses of dispatchable power) because, as mentioned above [28], converting electricity to hot water is justifiable only when there is an excess of electricity that could otherwise not be used. However, electric boilers with large capacities (up to the MW scale) still have relatively low investment costs and are to some extent compatible with existing DH schemes [29–31]. In contrast, heat pumps appear to be an attractive solution mainly because they use low-temperature heat, which makes them an efficient option, and they can be used as centralized units in DH systems if low-temperature waste heat is available [32]. Although electric boilers and heat pumps can exploit the thermal inertia of buildings and the sensible heat (hot water) in the DH system, such storage systems can cover demand-side variations only on a daily basis. In contrast, among the so-called indirect electrification alternatives, there are some that incorporate energy storage in the form of chemical energy. This is the case for the use of electricity to produce hydrogen that is stored and later used to produce heat [33]. This offers the possibility of greater decoupling (in time, but eventually also in location if the energy carrier is transported) between energy generation and demand, thereby solving the problem of adding an extra load to the electricity system and opening up opportunities to increase the penetration of VRE and potentially balance the instabilities of a future energy system. However, currently available technologies for storage and transportation of hydrogen require high-pressure tanks (up to about 700 bar) or chemical binding (with consequent increases in costs and safety measures—as well as the limitation related to the maximum reachable energy density, owing to the weight added) [34,35]. Depending on the energy system context, a few storage solutions can be combined to cover different types of variations, where TCES is especially suitable for long-term storage.

Not only would regional and national energy systems benefit from the electrification of heating services, as discussed above, but it should also be considered that energy use of biomass could become restricted. On the one hand, the price of biomass is likely to increase in the near term and midterm with expected increased competition for its use in other sectors. On the other hand, challenges related to obtaining sustainably produced biomass streams are foreseen. Although the importance and competitiveness of biomass-fired CHP in future energy systems have been highlighted in several studies as supporting

this technology to produce low-temperature heat, where they are preferred over electric boilers (a highly exergy-destructive process) [36], the increasing competition for biomass will probably result in that it will instead be used as feedstock to produce higher-value end products [37].

Along with this, new processes and technologies are steadily being advanced to enable the use of residual biomass streams in the chemical industry. At present, the production of hydrocarbons from renewables is high on the agenda for sectors in which it is challenging to substitute carbon-based commodities, such as in aviation, freighting, and the construction industry [38,39]. The EU Parliament has recently voted through an act to terminate the classification of some forest biomasses as carbon neutral, which if implemented would drastically limit the use of biomass for energy services. The situation is exacerbated by an expected shortage of biomass in the near future, as it is predicted that by 2030, the supply of forest biomass in Europe will be too low to meet the projected demand and that residual biomass will not be sufficient to bridge the deficit [40]. While the implementation of bioenergy with carbon capture and storage (BECCS) is planned as a carbon dioxide removal (CDR) technology, and specific targets are being proposed [41], it is not entirely clear how BECCS can economically compete and show a clear climate benefit with other uses of biomass in hard-to-abate sectors and for longer-lived products [42].

From the above background, we conclude that there will be a great need for storage technologies that can provide storage over longer time periods, from weeks up to seasonal storage. If such a system can be combined with the operation of a DH system, this could contribute to reducing the biomass dependency of production units in DH systems. Therefore, the aim of this work is to present and assess the concept of a TCES process that makes use of a redox loop, absorbs and stores VRE, and meets the varying demand of a DH system. For this purpose, the Swedish system is selected and used as a case study. This paper comprises the following: (i) a description of the proposed scheme (Section 2); (ii) a description of Sweden as a case study (Section 3); (iii) preliminary mass and energy balances at the plant level for the process scheme and for different future energy system scenarios in the context of the Swedish case (Sections 4 and 5); and (iv) a discussion of the practical implications, additional implementation options and opportunities and challenges associated with the suggested concept, including, to some extent, a comparison with potential alternatives for DH electrification (Section 6).

Although the case study in this paper focuses on the situation in Sweden to evaluate the concept, the work may also be relevant for other countries with DH systems that have characteristics similar to those in Sweden (plants of similar size and layout). The Swedish case constitutes an illustrative case thanks to its numerous DH systems and large reserves of metal ores. In Sweden, during 2020, out of the 49.1 TWh of DH delivered, 45% was produced in CHP plants, 33% in "heat-only" plants, and 11% from flue gas condensation in the CHP plants. In some Swedish cities, the use of industrial waste heat can constitute a large share of the base heat production. The main energy source is biomass combustion in the CHP plants [43], where only 9% and 1% of the heat is being supplied to the DH systems by heat pumps and electric boilers, respectively. Sweden has an advantageous starting point to develop an iron-based TCES system that is incorporated into DH systems. Sweden has had iron and steel production plants for a long time, and the national iron ore reserves are predicted to sustain operations beyond 2060. In addition, there is a planned transition to the electrification of industries (in particular the iron and steel industry) [44]. Along with the development of the iron production industry, the infrastructure to transport the ore is well established across the country, using the long coastline and navigable inland waters, and this makes it possible to supply densely populated areas that have a demand for DH.

2. The Proposed Scheme

This section describes the scheme proposed for a TCES process with the incorporated production of DH, based on a high-temperature redox cycle. The process absorbs nondispatchable electricity and stores it as chemical energy, which can subsequently be discharged as dispatchable heat. While the production of combined heat and power is a feasible option (discussed in Section 6.1), the DH-only scheme is the one assessed in detail in this work.

The primary scheme is depicted in Figure 1 and revolves around the possibility of retrofitting existing biomass-fired DH-generation facilities into high-temperature redox cycle TCES plants. The main components of the plant are the two gas–solid reactors, in which the metal is reduced and oxidized in a cyclical manner. FB reactors are recommended for both reactors thanks to their strong mass and heat transfer capabilities at a large scale and because current DH plants are often based on FB combustors; i.e., part of the already-installed infrastructure can be modified to perform the process described in Figure 1.
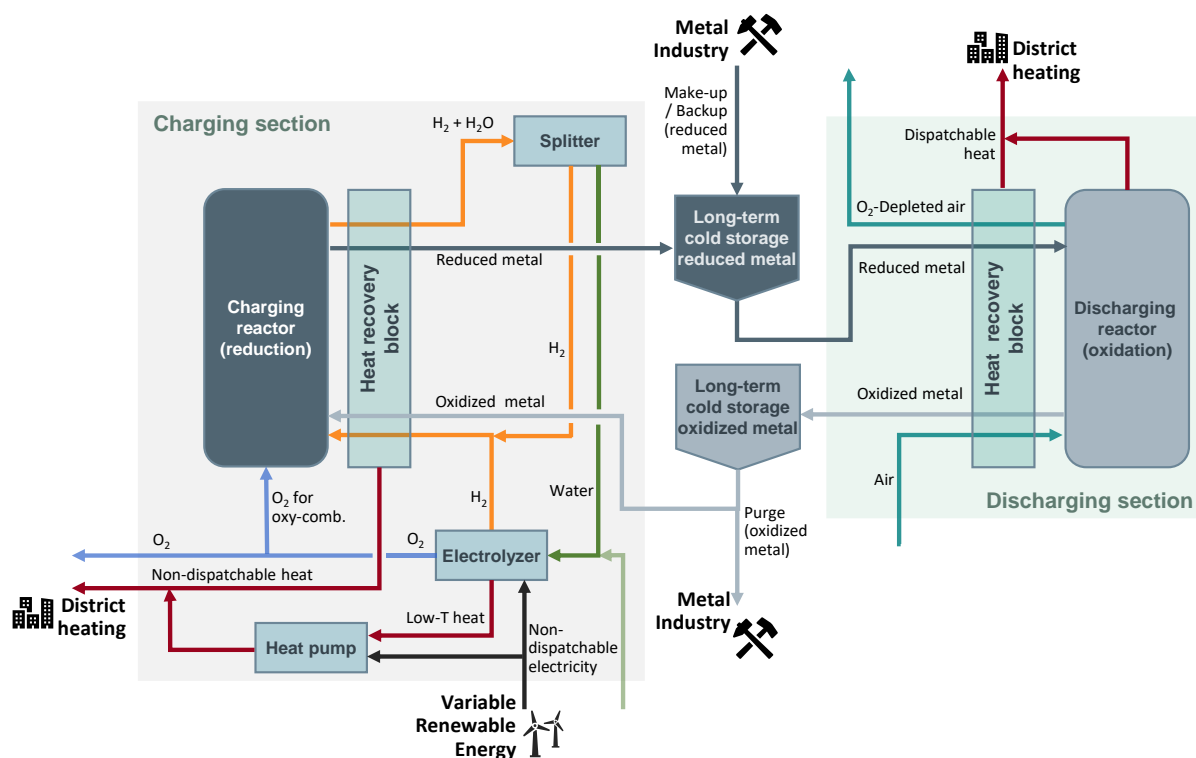
Figure 1. Schematic of the TCES plant proposed in this work, based on a high-temperature redox cycle. The plant absorbs VRE to produce hydrogen in the electrolyzer together with nondispatchable heat for the DH network. The hydrogen is then used to reduce a metal in a charging reactor. From there, the metal is transferred to a storage unit, from which the metal is subsequently transported to a discharging reactor, where it is oxidized to produce dispatchable heat for the DH network. A make-up stream of reduced metal is included, as is the purged oxidized material, which can be sent back to a local metal industry.

The charging section of the plant consists of low-temperature electrolyzers, the reduction reactor, a heat pump, and the storage tank(s) for the reduced material. The electrolyzers absorb renewable electricity in order to split water into molecular oxygen and hydrogen. The latter is fed to the reduction reactor, where the chemical reduction of the metal oxide occurs. Because the net reduction reaction is endothermic, an additional input of energy is required to complete the reduction reaction of the solid material [45]. To meet this requirement, additional hydrogen (around 20% compared with the amount needed for the reduction) must be generated by electrolysis, so that it can be oxy-combusted in

the reduction reactor. Note that the amount of additionally needed hydrogen can be reduced by recirculating the exhausted fraction (after separation from water) from the reactor, the amount of which is defined by the thermodynamic equilibrium under the conditions of the reaction. The hot streams exiting the reactor are used to preheat the inlet streams, which leaves a surplus for the further extraction of heat in the form of DH. Similarly, the heat losses from the electrolyzer (up to 30% for alkaline units) can be used for this purpose. As the charging section is operated during periods when electricity is available at prices that are competitive for the process, a heat pump can be installed to further recover the low-temperature heat losses and shift them to DH temperatures. Thus, the operation of the charging section involves the associated production of nondispatchable DH (see the operational modes in Figure 2).
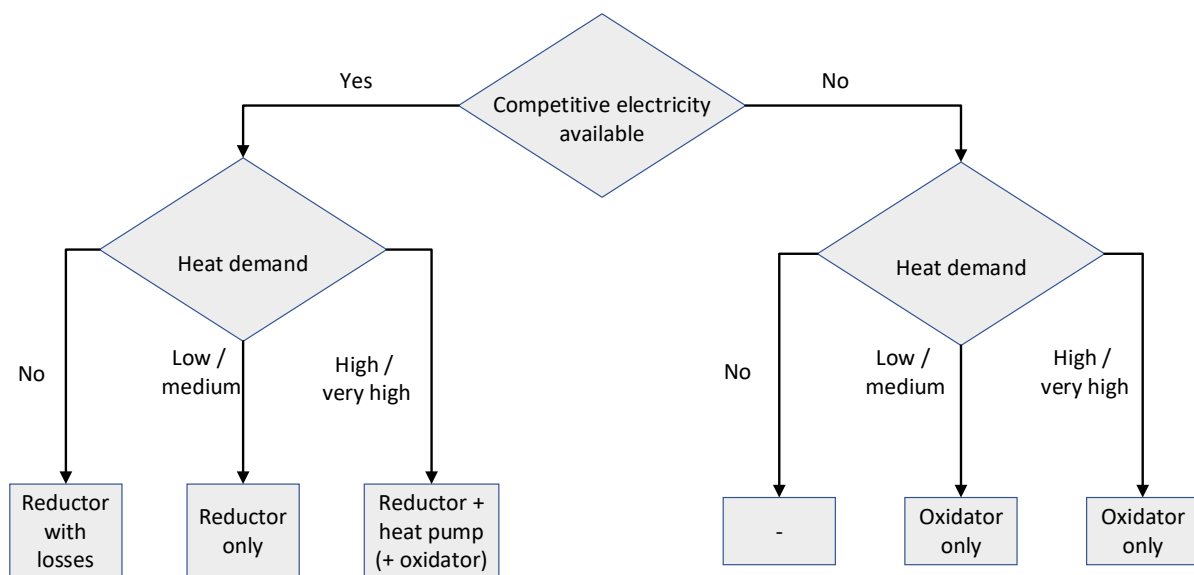
Figure 2. Schematic of the TCES plant proposed in this work, based on a high-temperature redox cycle. The plant absorbs VRE to produce hydrogen in the electrolyzer together with nondispatchable heat for the DH network. The hydrogen is then used to reduce a metal.

Regarding the discharging section, reduced material from the corresponding storage tank(s) is fed into the oxidation reactor, where air is used to fluidize the solid material while providing the required oxygen for oxidation. The heat liberated during the reaction is absorbed by membrane tube walls (available in existing boilers), thereby generating steam that can be further utilized for heat production according to the conventional schemes (i.e., desuperheating and condensation), which are also present in the retrofitted plant. Thus, whenever it is operated, the discharging section produces dispatchable heat at the desired temperature level. The heat exchange between the inlet and outlet reactor streams is crucial to maximizing the energy efficiency of the discharge section.

Because the operations of the reduction and oxidation reactors are decoupled through the addition of solid storage at ambient temperature, the sizing of the reactors (as presented in Section 4) can be designed so that the charging section operates only during periods of strong availability and competitive prices of renewable electricity (hereinafter referred to as *competitive electricity*), while the discharge section can be dispatched on the basis of demand for heat, i.e., following the same operational pattern as that applying to DH boilers operated today [46]. Nonetheless, there may be periods during which the heat demand can be covered by the charging section alone, as this section generates a considerable amount of nondispatchable heat. Thus, the proposed scheme increases the plant heat-generation capacity, and the use of the oxidation reactor can be reserved for periods of high heat demand and noncompetitive electricity prices. Thus, several operational modes can be defined on the basis of the availability of competitive electricity and the

demand for heat, as displayed in Figure 2. First, as the additional heat production is non-dispatchable, its utilization is prioritized, and the heat demand should as a matter of priority be covered by the nondispatchable generation. The possibility to boost heat production is also enhanced by the installation of a heat pump, which can be used to recuperate the heat losses generated while reducing the metal. In addition, operating both the reduction and oxidation sides is possible under conditions of very high heat demand and competitive electricity prices.

A purge and a make-up stream of solid material are required owing to the expected loss of reactivity, attrition (due to structural changes caused by repeated extreme temperature changes) and consequent elutriation and to melting or sintering, among others. The need for make-up depends largely on the mechanical performance of the material and the reaction conditions, which are specific to the redox system used. In this regard, the redox system may be chosen based on the availability of metals or ores in the region or country in question, which contributes to a synergy between the storage plants and the metallurgic industry. The make-up solids would be supplied by the metal mill and transported using the existing infrastructure, whereas the depleted solid material could be sent back to the metal industry. A buffer of fresh solids can be kept at the metal mill for periods of constant high electricity prices or peaks in the heat demand that cannot be covered by the storage on-site. At the same time, the metal reduction industry could benefit from the expanded, distributed capacity for ore reduction offered by the retrofitted storage plants while maximizing the utilization of the low-temperature heat produced during the reduction process.

A key aspect of the proposed scheme is that all the essential pieces of process equipment used in the scheme are available at the large scale, which means that there is a low risk that the process will be hindered by a lack of suitable equipment. While the oxidation of metal fuels with air has been studied for several decades [47], technology for the full reduction of metals with hydrogen in FB reactors at the MW scale has been developed by Metso Outotec and Exxon/SiemensVAI [48–50]. Although a major challenge linked to these processes is the very high degree of reduction required in the output solids stream [51], the current concept proposes a redox cycle involving degrees of reduction that are more easily attainable and that require simpler process layouts. Alkaline electrolyzers are currently undergoing rapid refinement and expansion in terms of the number of installations and reduced costs, and they are available up to the GW scale [52]. The novelty of the proposed TCES scheme is that it combines already-existing processes into an entirely new configuration. Thus, although the proposed TCES is novel, it should be possible to implement it at a high technology readiness level (TRL).

3. Sweden as a Case Study

In the present work, Sweden is selected as an illustrative case to carry out an initial assessment of the proposed scheme. As explained in Section 1, Sweden has strong potential to implement such a system thanks to its existing metal ore mining activity and infrastructure for metal reduction, the ongoing expansion of VRE electricity, and widespread DH systems.

Fe-oxide systems should be suitable as TCES materials due to the high energy density of metallic iron, the good availability of the ores, competitive cost, and the availability of a considerable body of research and data on the characteristics of the Fe-oxides [53]. The latter is linked to the fact that the reduction (and, partially, the oxidation) of iron has for decades been the subject of study in metallurgy. More recently, the cyclic reduction/oxidation of iron and iron perovskites has received attention thanks to research on chemical looping combustion (CLC) processes [54]. The volumetric energy density of pure iron, assuming full oxidation, is 40.7 MJ/L, which is considerably higher than that of wood (about 3 MJ/L) or coal (range of 26–49 MJ/L), and significantly higher than that of hydrogen (5.3 MJ/L) [55] (see Figure 3). Note that the gravimetric energy density of iron is very low compared with that of H_2: 5.2 MJ/kg versus 141.8 MJ/kg, respectively. However, storing hydrogen requires high-pressure tanks or

chemical binding, which reduces the gravimetric energy density. Additionally, depending on the degree of reduction and the particle size of the iron powder, its volumetric energy density can be reduced by up to 50%.
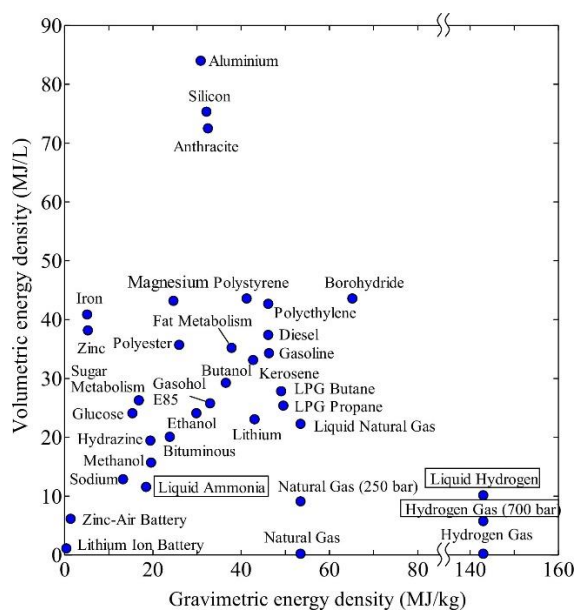

Figure 3. Gravimetric and volumetric energy densities of metals compared with organic combustible materials and batteries. Source: Kobayashi et al. [55].

Iron can be thermally reduced by heating the ore to the decomposition temperature of the oxides [56], or it can be chemically reduced in the presence of a hydrocarbon, CO, or H_2 (significantly lowering the temperature of reaction). The iron and steel industry has traditionally used coal in the reduction process (which is gasified in an oven to produce reductant species). More recently, the direct iron-reduction (DIR) process [51] has attracted attention mainly because it employs natural gas instead of coal (which is reformed during the process), thereby lowering the carbon emissions of the process. The DIR process is based on a multiphase reaction between small particles of the ore and gaseous H_2 and CO to produce "sponge iron", which can be subsequently melted in an electric arc furnace (EAF). This is regularly performed in FB reactors, and it omits the pelletization step, which was traditionally needed when using coal. One recent advance in the iron-reduction process is the use of pure hydrogen as the reduction agent [57,58], which completely excludes the participation of carbon atoms and eliminates the CO_2 emissions attributed to the reduction process. The hydrogen employed in the process should be produced via electrolysis by using renewable electricity. This process has been proven to be technically feasible at the large scale (where FB-based processes provide outputs in the range of 0.5–2.0 Mt/yr once having been implemented [48]). Sweden, in line with the latest national plans for decarbonizing steel production, is advancing toward the industrial implementation of such a process [59].

The process presented in Section 2 is amenable to implementation in any existing combustion-based DH plant that uses the FB technology, which is the most commonly used firing technology in Swedish DH systems. The typical capacities of such plants are around 100 MW thermal output [60], which is the reference plant size considered in the present work (see Section 4.2). From the national perspective, if a sufficiently high number of plants is retrofitted according to this scheme, a firm connection between the iron industry and the DH network will be created (depicted in Figure 4). The retrofitted DH plants would make use of the stored DRI available at the iron mill site to (i) supply the required make-up flows of iron and maintain a high degree of cyclability within the DH plants and (ii) cover the periods of unexpected peaks in the heat demand. Correspondingly, the

material purged from the DH plants is sent back to the iron mill, which could be reutilized for steelmaking. The retrofit of the DH system will then lead to a substantial increase in the total inventory of the stored DRI, possibly leading to greater flexibility in the iron and steelmaking processes. Regarding the transport of reduced iron from the metal mill (in the northern region of Sweden) to each DH plant (and vice versa), populated coastal areas would benefit from the possibility to transport by ship, whereas regions without access to harbors would rely on land-based transport options, such as trains and trucks. A detailed analysis of the logistics (train and road routes, distances to harbors from each plant, etc.) of transporting DRI is outside the scope of the present paper.
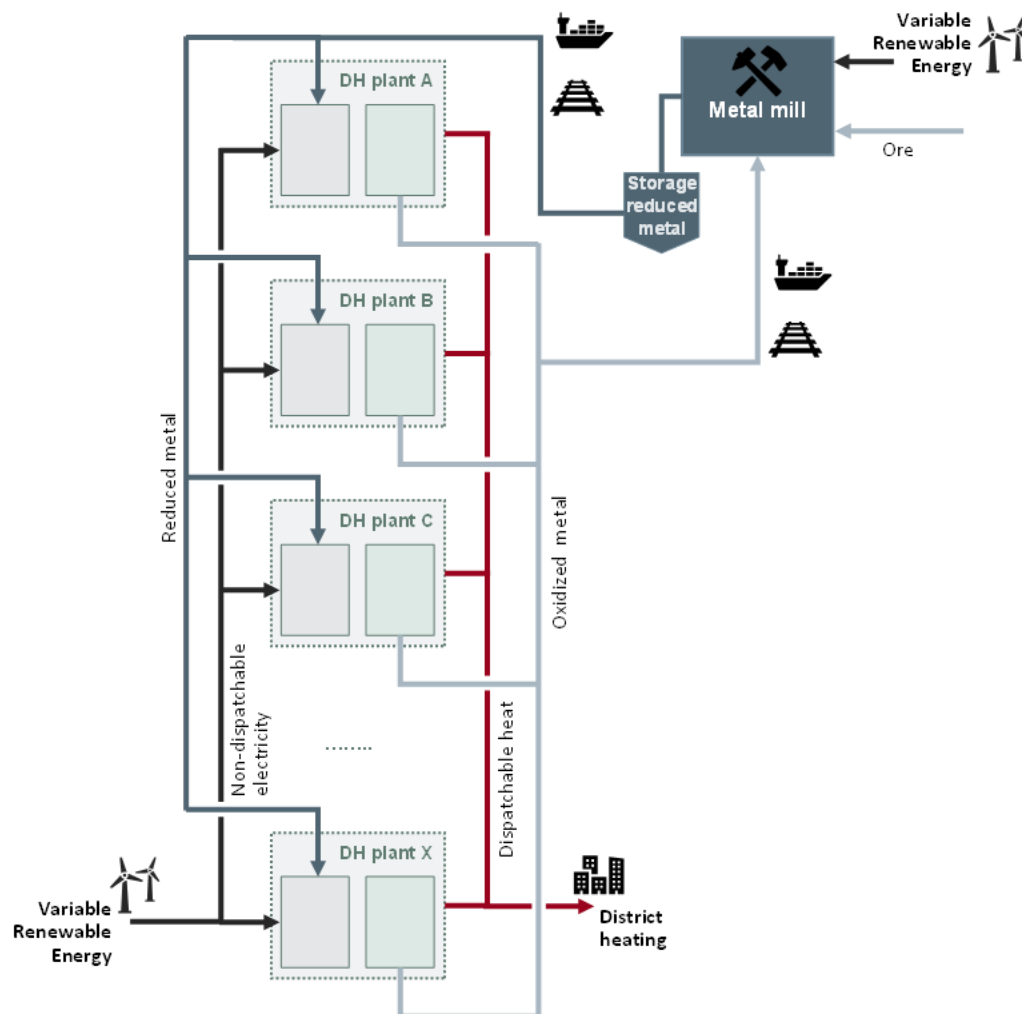

Figure 4. Scheme at the national level for the storage of energy and production of DH from renewable electricity using an iron redox cycle. The iron mills, located in the northern region of Sweden, maintain a backup storage system for reduced iron, which can be used for make-up or to cover unexpected peaks in the heat demand. Depleted iron oxide is sent back to the iron mills. The transportation of iron relies on the transport infrastructure and logistics already provided by the iron industry.

4. Methodology

4.1. Overview

The present work comprises a quantitative assessment of the proposed scheme by using exclusively energy and mass balances at the plant level. An overview of the assessment methodology is presented in Figure 5, where the inputs and outputs for the calculation of the energy and mass balances are indicated. By selecting certain geographic and temporal contexts, the input parameters can be defined, i.e., the redox system, the

representative plant size, the electrolyzer type, and the surrounding energy system. The latter will define the availability and variability of electricity at a certain price profile, a share of which can be used and stored within the system. Note that the process is based on the retrofitting of existing units, as does the methodology presented in Figure 5.
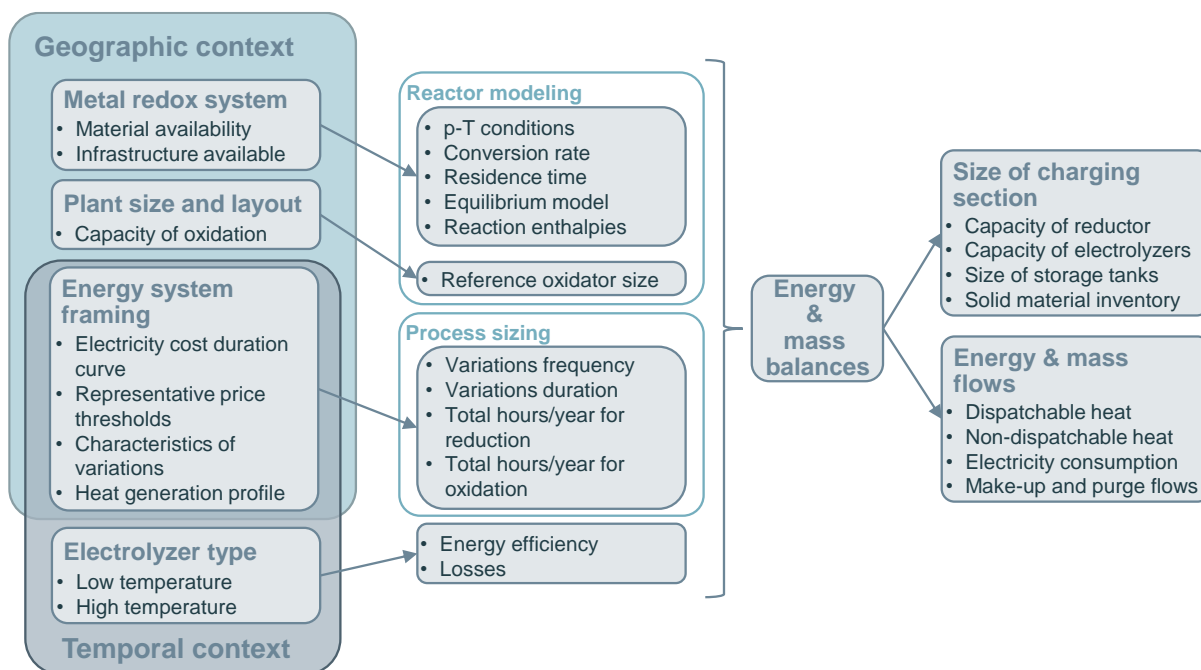
Figure 5. General methodology followed to assess the suggested scheme in given geographic and temporal contexts.

4.2. Considerations for the Case Study

Preliminary mass and energy balances are computed for an existing reference DH plant with an installed thermal output capacity of 100 MW, retrofitted according to the process described in Section 2. The chosen reference capacity corresponds to that of a typical size of plant with biomass-fired FB boilers in Sweden [60]. The metal system selected for the case study is iron, as explained in Section 3. The characteristics of a possible future electricity market in terms of generation technologies and corresponding annual price profiles (including variations thereof) are considered through the selection of nine scenarios, as described in Section 4.2.1.

4.2.1. Framing of the Energy System

The reference DH plant is assumed to be operated as a base-load unit in a local municipal DH system. For simplicity, it is assumed that the plant is dispatched for full-load operation during the winter months, i.e., 6525 h/yr, and is switched off during the summer (a common practice when assessing this type of plant [46]), as shown in Figure 6. Different electricity price profiles (on-spot production electricity prices) are used to evaluate the impact of electricity availability, which is reflected in the capacities of the electrolyzers and reduction reactor, as well as its variability, which will affect the storage size. The present work considers different electricity price profiles simulated by the electricity system investment model "hours-to-decades" (H2D) [33]. This model minimizes the investment cost of the electricity system for three scenarios (corresponding to three carbon tax rates) while meeting the corresponding foreseen electricity demand of Northern Europe, subdivided into 12 regions to represent major transmission bottlenecks. Thus, the optimum technology mix for electricity generation, transmission, and storage capacities is identified. This work uses three electricity price profiles for the south of Sweden, which are obtained from the model by representing different ratios, from wind power to nuclear

power (derived by simulating Years 2030, 2040, and 2050, respectively, in the aforementioned region). Table 1 lists the resulting electricity mixes and the corresponding assumed CO_2 tax for each price profile. For a deeper insight into the electricity profiles utilized, the reader is referred to [33].
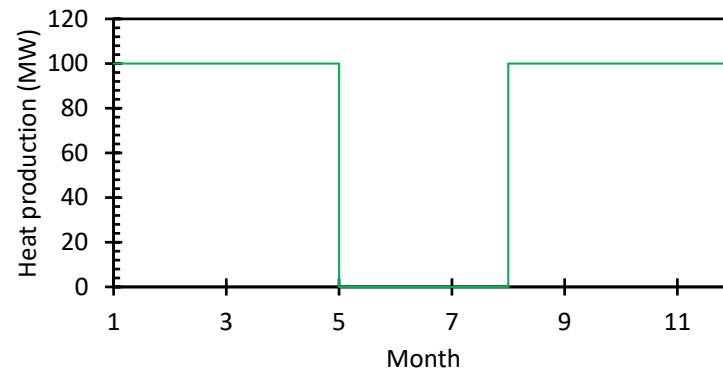
Figure 6. Amount of dispatchable heat production over the year assumed to be generated at the reference DH plant.

Table 1. Electricity mixes and cost of CO_2 tax for the three electricity price profiles considered. Notes: CCGT, combined cycle gas turbine; PV, photovoltaic.

Electricity Price Profile		A: Nuclear_Dominated	B: Medium_Wind	C: High_Wind
Electricity mix (%)	Hydro	12	20	27
	Wind	31	52	65
	Nuclear	56	27	-
	PV	1	1	2
	Biogas			
	CCGT	-	-	6
CO_2 tax (€/tonne)		40	100	400

The present work does not make cost optimization calculations for sizing the TCES process. Instead, for a given electricity profile, three thresholds in relation to the electricity price for triggering the charging section of the TCES process are selected (i.e., varying what is considered competitive electricity for the process), corresponding to the different operation hours of the charging step:

- Price threshold 1, *Only_VRE*—the charging step makes use of only wind-dominating periods.
- Price threshold 2, *UF_50*—the charging step utilizes electricity for 50% of the year.
- Price threshold 3, *No_peak*—the charging step avoids only peak price events, characterized by sharp increases in the price duration curves.

Each threshold is, therefore, applied to each price profile. The resulting nine scenarios are presented in Table 2, such that each one has a specific electricity price level (i.e., considered competitive electricity), above which the charging section is never turned on, corresponding to a reduction running time, t_{red} (hours per year that the charging section operates), utilization factor (UF, which is calculated for the charging section), and average duration of variations (ADV, [46]). The ADV is computed as the weighted average of the duration of the periods in which the price rises above the threshold. As shown in Table 2, the ADV of the *Only_VRE* threshold is the largest for all three price profiles, as it represents periods with typical durations of variations of 7–12 days [46]. The ADV of the *No_peak* threshold is shorter than 12 h for all the scenarios, as it represents daily peaks of high demand, while the ADV of the *UF_50* threshold is intermediate to those of the other two thresholds.

Table 2. Characteristics of the nine scenarios considered in this work. The parameters are calculated according to the characteristics of the electricity price profiles and the criteria formulated for the selection of thresholds. UF, utilization factor; ADV, average duration of variations.

Threshold/Electricity Price Profile		A: Nuclear_Dominated	B: Medium_Wind	C: High_Wind
Only_ VRE	Reduction running time, t_{red} (h/yr)	1487	1680	5295
	UF (-)	0.17	0.19	0.60
	ADV (h)	181	244	147
UF_50	Reduction running time, t_{red} (h/yr)	4380	4380	4380
	UF (-)	0.50	0.50	0.50
	ADV (h)	54	64	90
No_peak	Reduction running time, t_{red} (h/yr)	8605	8596	8502
	UF (-)	0.98	0.98	0.97
	ADV (h)	12	7	8

The electricity price for each scenario is not presented here, because it has no impact on the calculation (as the performed process sizing is a function of UF and ADV). This is the case because, as mentioned before, the electricity price profiles correspond to production prices, which differ from the actual buying prices, which for industries are typically based on some price-purchasing agreement (PPA), i.e., a more or less long contract. The present assessment addresses the impacts of the variations and operational mode on the net energy and mass balances over the process, rather than the impact of the absolute value of the electricity price. As a consequence, the results are limited to reflect how the TCES process performance depends on the dynamics of the electricity price curves.

4.2.2. Process Sizing

The present work performs the plant sizing required for the oxidation reactor to provide dispatchable heat during the cold months of the year, as it does before the retrofit. Note that this will most likely result in excessive capacities for the charging section, as the installation of the charging section adds a certain nondispatchable heat-generation capacity to the process. Nonetheless, it represents the most conservative situation in which, given an electricity mix and a price threshold (see Section 4.2.1), the plant can ensure dispatchable heat generation throughout the year (for an overview on the plant operational map, see Figure 2). Thus, the oxidation reactor is assumed to steadily operate for 6525 h/yr (from 1 September to 31 May), where the solid inflow and solid outflow, $F_{oxid,in}$ and $F_{oxid,out}$, respectively, are computed from the energy and mass balances over the reactor (see Section 4.2.3). In contrast, the reduction reactor operates intermittently but at full capacity whenever it is in operation, during t_{red} h/yr. Thus, in comparison with the oxidation reactor, the reduction reactor capacity is overdimensioned because it needs to provide sufficient reduced solids to cover the periods during which it may not operate. Thus, the capacity of the reduction reactor (expressed as solid inflow, F_{red}) is computed according to Equation (1):

$$F_{red,in} \cdot t_{red} = F_{oxid,out} \cdot 6525 \qquad (1)$$

In this paper, the sizing of the storage is calculated as a function of the *ADV*, according to Equation (2). Instead of optimizing the sizing of the storage so that it can cover all the possible variations in a given year (as is common in other storage systems; see, e.g., [61]), a backup at a metal mill, which is located in the northern part of the country and available at all times, is assumed here (see Section 3). Thus, the storage size is here

calculated for each of the nine scenarios on the basis of the types of variations that must be absorbed, i.e., to cover periods with a duration of *ADV* h.

$$M_{solids,stored} = F_{oxid,in} \cdot ADV \tag{2}$$

In order to quantify the share of dispatchable heat in the total heat generated after the retrofit, a dispatchability ratio r_{disp} is defined according to Equation (3). This factor represents the fraction of the absorbed VRE that can be delivered with a displacement in time (and potentially in space), i.e., how much of the consumed electricity is actually stored. Such a metric is relevant for comparing the proposed scheme with other alternatives for the electrification of DH and for the evaluation of different configurations of this same process.

$$r_{disp} = \frac{Dispatchable\ heat}{Dispatchable\ heat + Nondispatchable\ heat} \cdot 100 \tag{3}$$

Although the proposed scheme is suggested to operate with low-temperature electrolyzers (see Section 2), this work includes two types of electrolyzers in the assessment: a low-temperature electrolyzer operating with liquid water at 90 °C and a high-temperature electrolyzer operating with steam at 900 °C [62]. This is to include a future scenario in which the high-temperature electrolyzer technology is assumed to be available, which will facilitate heat integration [63]. It is assumed that 60% of the losses from electrolyzer are recoverable (this number is higher for the case with a low-temperature electrolyzer if a heat pump to enable the recovery of the heat losses at a temperature that is useful for DH is installed), which is an assumption line with [62].

Lastly, the cyclability of the material is estimated on the basis of the experimental results from a 100 kW CLC unit that applied redox cycles similar to those envisioned here [64]. From the results, it was concluded that iron oxide materials can sustain 2000–5000 cycles ($N_{lifetime}$) of high-temperature oxidation reduction before being elutriated from the reactors (this is assumed to occur at a faster rate than that of the chemical deactivation of the material). Thus, the make-up and purge flows are here computed according to Equation (4), which computes the residence time of each cycle based on the sum of the residence times of each volume involved (i.e., the reactors and storage tanks). Some additional process parameters utilized for the mass and energy balances, as well as for the storage sizing, are displayed in Table 3.

$$\dot{m}_{make-up} = \frac{M_{system}}{N_{lifetime} \cdot \tau_{cycle}} \tag{4}$$

Table 3. Process parameters used for the energy and mass balances.

Parameter	Value
Low-temperature electrolyzer electricity consumption	194 MJ/kg$_{H2}$
High-temperature electrolyzer electricity consumption	136 MJ/kg$_{H2}$
FeO density	5740 kg/m³
Fe$_3$O$_4$ density	5170 kg/m³
Fe$_2$O$_3$ density	5240 kg/m³
Void fraction of bulk materials	0.5 (-)
Lifetime of the material, Nlifetime	3500 cycles

4.2.3. Reactor Modeling

The oxidation and reduction reactors are modeled in Aspen Plus as RGibbs reactors, i.e., by assuming chemical equilibrium and on the basis of the Gibbs free energy minimization model [65] (see Table 4). The reactor models allow for Fe(s), FeO(s), Fe$_2$O$_3$(s), and Fe$_3$O$_4$(s) as possible solid species in the equilibrium. Following the analysis carried out by Bahgat et al. [66], the conditions in the reduction reactor are fixed at 1100 °C and 1 bar,

such that the degree of reaction is maximized for a relatively low reaction time (i.e., 100 min). Because the reduction of Fe_3O_4 is the slowest reaction [67], its molar concentration in the solid phase at the outlet of the reduction reactor is fixed at 10% of Fe_3O_4. The net heat requirement of the reduction reactor is supplied by combusting additional hydrogen (above that required for establishing the equilibrium of the reduction reactions), which is also supplied by the electrolyzers. The combustion is assumed to occur prior to the reduction chamber (with an efficiency of 98%), and therefore, the molecular oxygen is assumed to be not present for the reduction reaction and does not need to be accounted for in the equilibrium. Thus, the total H_2 production of the electrolyzers is the sum of the reduction requirement, $H_{2,red}$, and the combustion requirement, $H_{2,comb}$. Regarding the oxidation reactor, conditions similar to those in an air reactor used in CLC research [47] are selected, i.e., 900 °C and 1 bar, under the assumption of no FeO in the outlet stream (as it is the limiting oxidation reaction step).

Table 4. Reactor operational conditions, given parameters, and outlet condition constraints.

Reactor	Operational Conditions	Given Parameter	Outlet Condition Constraint
Reduction	1100 °C and 1 bar	Solids inflow	10% Fe_3O_4 content in solid phase
Oxidation	900 °C and 1 bar	Net heat flow	0% FeO content in solid phase

In addition, the following assumptions are made when modeling the reactors:

- Uniform pressure and temperature are assumed.
- No pressure or heat losses is assumed.
- Steady-state operation is assumed.
- The solid streams entering each reactor are assumed to be heated to a temperature that is 200 °C lower than the reactor temperature, through a series of heat exchangers that recover heat from the outlet reactor streams. This assumption is on the conservative side according to the results from equivalent works [68].

5. Results

The energy and mass balances of the process applied to the Swedish case were calculated for each of the nine scenarios specified in Table 2, which correspond to different combinations of electricity price curves (representing different generation technology mixes (A.B.C.) and ADV values in the range of 7–244 h) and price thresholds (that translate into UF values in the range of 0.17–0.98). After the overall energy balance has been assessed, the results are presented in terms of the size of the iron storage; capacities of the reduction reactor and the electrolyzers; and electricity and solid material make-up requirements. For each case, an assessment of the process with high-temperature electrolyzers is also carried out. The chemical compositions of the solid streams indicate that while the solid stream leaving the oxidation reactor is composed of 100% Fe_2O_3, the material exiting the reducer is a combination of FeO (74%) and Fe_3O_4 (26%), which suggests that metallic iron cannot be generated under the reduction conditions present in the reduction reactor. This outcome does not depend on the scenario, given that the reaction conditions are identical for all the computed scenarios.

Figure 7 shows the overall energy balances of the proposed scheme for both of the charging and discharging sections, normalized for 100 energy units of dispatchable heat production, for the processes with low- and high-temperature electrolyzers. A look at the charging section shows that despite the fact that a large share of the heat losses from the electrolyzers is recovered by the heat pump, unrecoverable losses persist and make up the largest fraction of the losses in the system. It is also clear that the reduction reactor suffers no heat losses, thanks to the placement of the heat pump, while the oxidation reactor has an 8% inherent loss of heat because no heat pump is assumed available when running the discharging section (although this aspect could be considered in further analyses, it would be subject to the availability of competitive electricity). Regarding the case in which high-

temperature electrolyzers are used for the retrofit (Figure 7b), the fraction of the heat losses slightly increases compared with the process with low-temperature electrolyzers, owing to the absence of the heat pump, whereas the level of electricity consumption is substantially decreased.
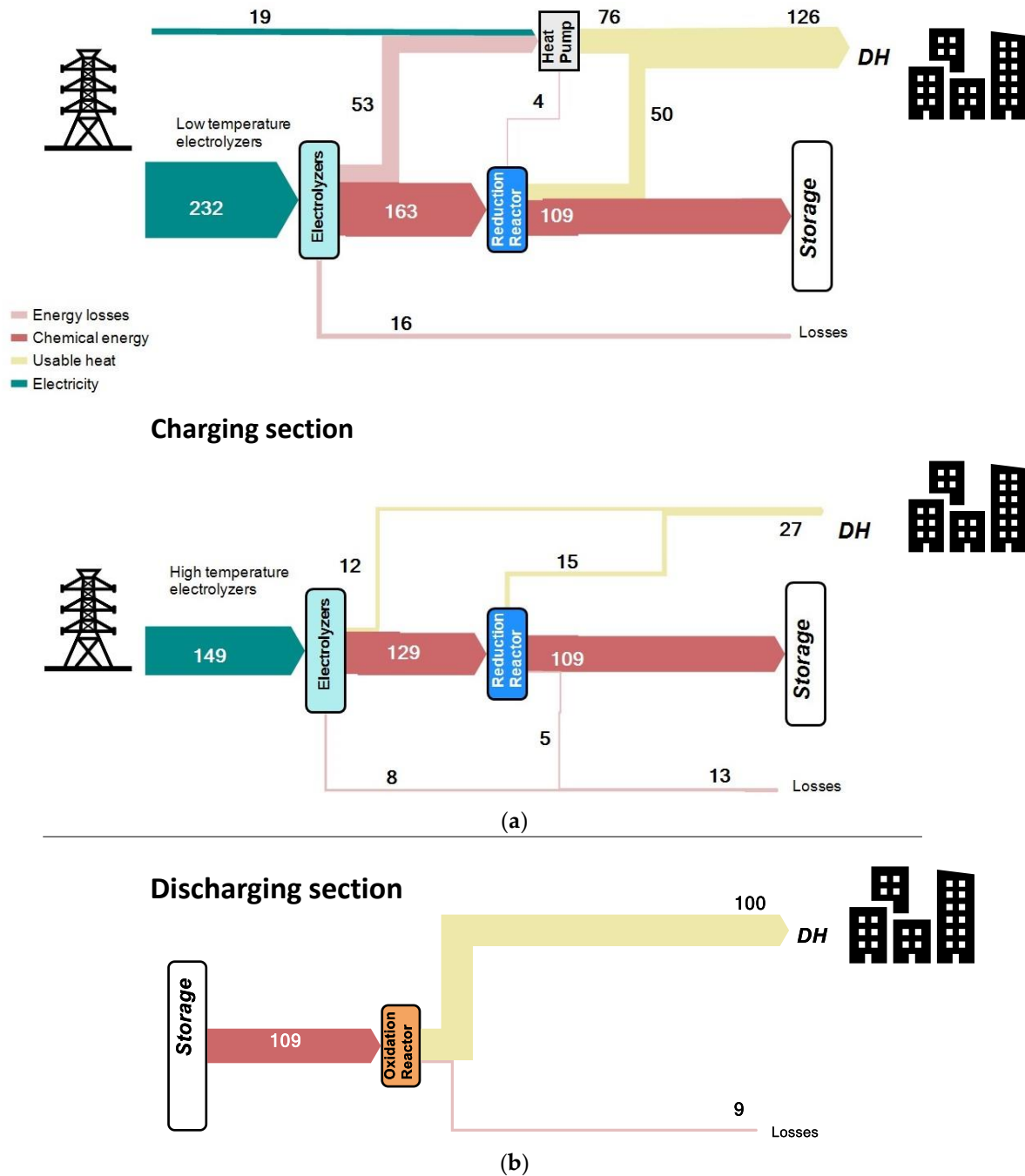
Figure 7. Overall energy flows of the proposed scheme for both the low-temperature electrolyzers case and the high-temperature electrolyzers case, normalized for 100 energy units of dispatchable DH production (i.e., generated in the discharging section). Note that the discharging section in the case with high-temperature electrolyzers is the same as that in the case with low-temperature electrolyzers and, therefore, is not included (**a**) Energy flow of the charging section for the schemes with low-temperature electrolyzers (top) and with high-temperature electrolyzers (bottom) (**b**) Energy flow of the discharging section (does not differ between the two electrolyzers).

In fact, the calculated levels of electricity consumption do not differ among the nine scenarios (Table 2), although they are heavily dependent on the type of electrolyzer used,

being around 1.8 TWh/yr for the low-temperature electrolyzers and 1.1 TWh/yr for the high-temperature electrolyzers (Figure 8). According to a comparison of these values with the annual heat production levels of the plants (1.67 and 0.94 TWh/yr, respectively), the computed energy efficiencies of the processes turn out to be around 90% and 86%, respectively. Importantly, the approach taken in this work to compare setups is based on the assumption of a retrofit of current plants, where the FB biomass boiler is converted into an iron oxidation reactor that is capable of running at maximum capacity for 6525 h/yr. Consequently, as shown in Figure 8b, while the total amount of dispatchable heat generated in the oxidation reactor remains the same for both cases (and equivalent to the level of heat generation of the original plant), there is an added nondispatchable heat production that differs between the low- and high-temperature electrolyzer cases. Thus, there are substantial differences in the share of dispatchable heat as compared with the total heat generated, where r_{disp} is 44% and 79% for the low- and high-temperature electrolyzer cases, respectively. This is due to the much higher level of nondispatchable heat delivered in the reduction section for the case with low-temperature electrolyzers, as a consequence of their having higher electricity consumption. The maximum fraction of nondispatchable heat that can be recovered from the reduction side of the low-temperature electrolyzer case if a heat pump is in place is indicated in Figure 8a with a dashed yellow line. To aid the comparison (see Section 6) of the suggested scheme with other heat production electrification alternatives, Figure 8 includes the values estimated for the heat generation, electricity consumption, and energy efficiency of a heat pump–based system delivering 100 MW_{th} of DH.

(**a**)   (**b**)
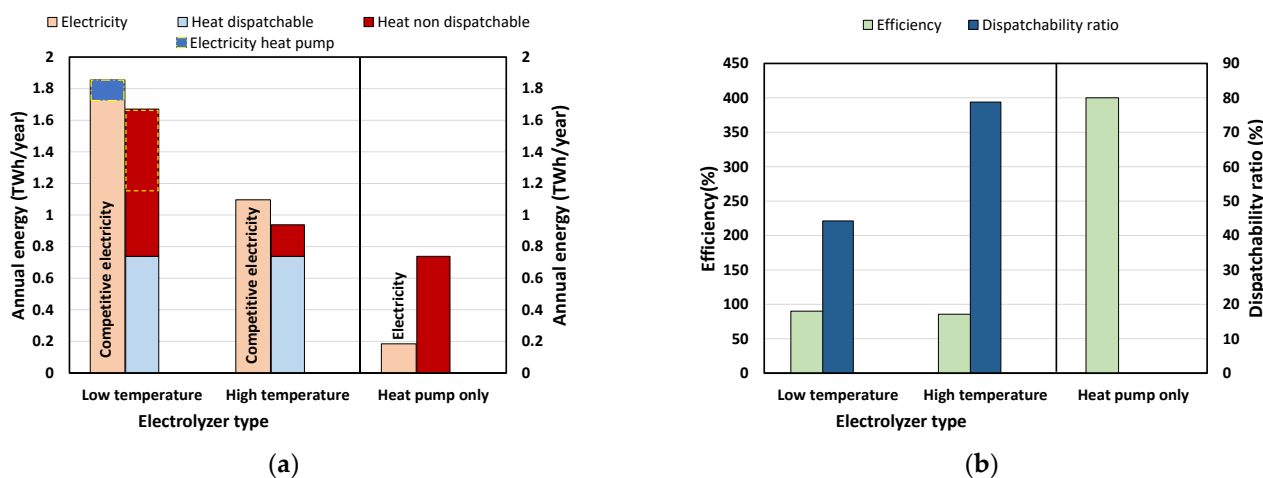
Figure 8. Energetic performances of the investigated process for the two types of electrolyzer units considered. For comparison, the estimated performance of an equivalent DH heat pump system is included (note that against the TCES process, heat pump only does not consume exclusively competitive electricity and therefore is indicated as "electricity") (**a**) Annual net energy flows of the proposed scheme for the two types of electrolyzers analyzed. The dispatchable heat is generated in the discharging section, while the nondispatchable heat is generated in the charging section. The amount of nondispatchable heat that can be recovered if a heat pump is in place is marked within a dashed yellow line (**b**) Dispatchability ratios and energy efficiencies (electricity to heat) of the proposed scheme for the two types of electrolyzers analyzed. Note that the dispatchability ratio of heat pump only is 0.
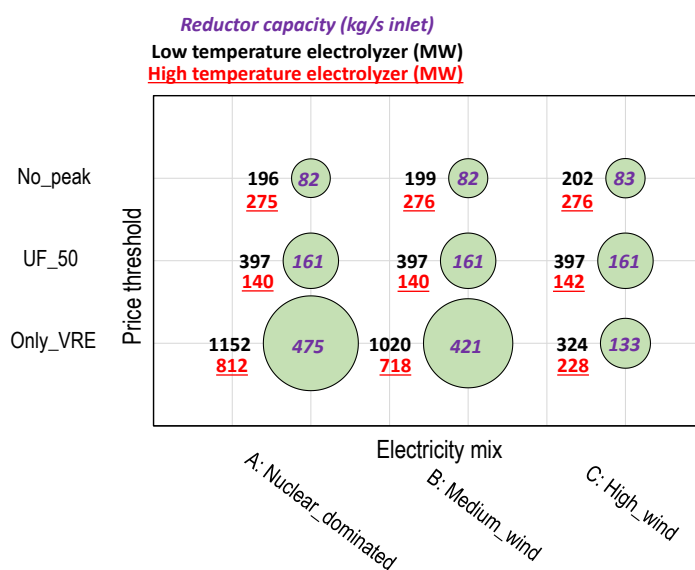
The computed inventories of the reduced solid materials (in tonnes) and the sizes of the storage silos (in m³) are shown in Figure 9. The required stored material linearly correlates with the ADV. Therefore, the required storage is largest for the *Only_VRE* threshold (52,534–87,199 tonnes), while the *No_peak* threshold requires the smallest material inventories (2500–4200 tonnes), as only electricity demand peaks with durations of 7–12 h are to be covered by the storage. Translating the masses of stored solids into volumes, the

Only_VRE threshold requires a tank for the reduced solids with a volume of 18,000–30,000 m³, whereas for the *No_peak* threshold, a tank with a volume of around 1000 m³ is needed. Note that in all the scenarios, a second storage tank of similar size is required for the oxidized material. As expected, the results computed for the *UF_50* threshold lie somewhere in between those for the other two thresholds for all the investigated scenarios. The computed tank sizes can be compared with conventional tanks found in process facilities such as refineries, which range in volume from 10,000 to 100,000 m³ for a single tank.
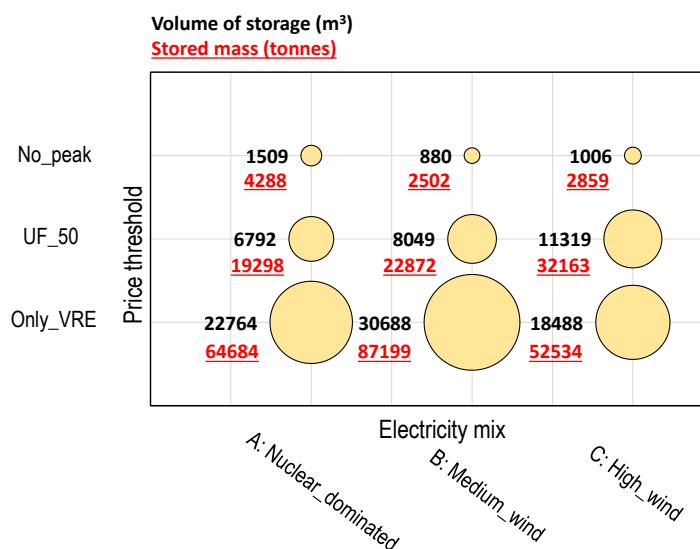

Figure 9. Sizes of the inventories of reduced material required (in tonnes) and the corresponding storage volumes, for the nine scenarios under investigation.

The required installed capacities of the reduction section units are plotted in Figure 10, in terms of the power capacities of the electrolyzers (MW) and the mass inflows of solids for the reduction reactor (kg/s). Note that both variables correlate directly with the reduction running hours, which means that the scenarios computed for the *Only_VRE* threshold again show the largest capacities. However, for the *High_wind* profile, the required capacities are reduced while keeping the operational costs low (as *Only_VRE* represents the threshold with electricity at the lowest prices). It can also be seen in Figure 10 that, as expected, the *No_peak* scenarios result in the smallest capacities, as the UF value of the reduction section is kept close to 1. When utilizing low-temperature electrolyzers, the computed capacity to be installed is in the range of 196–1150 MW, while the capacities of the more efficient high-temperature electrolyzers are on average 30% smaller, in the range of 140–812 MW. The reduction reactor's inlet mass flow is between 82 kg/s for a UF value close to 1 and 475 kg/s for the scenario with the lowest UF value (0.17). Note that for the scenarios with the *No_peak* threshold, the capacity required for the reduction reactor is smaller than that required for the oxidation reactor (with an inlet solid flow of 108 kg/s). This is because with storage in place, the reduction section is allowed to operate during the summer months, in which case the oxidation reactor is turned off, therefore yielding a larger t_{red} value than the case without storage. Nevertheless, for such a case, an additional inventory of solids would be required because the reduction reactor should be able to run independently of the oxidation reactor during the summer months.

Reductor capacity (kg/s inlet)
Low temperature electrolyzer (MW)
High temperature electrolyzer (MW)

Figure 10. Capacities required for the electrolyzers (in MW, including both the high- and low-temperature cases) and the reduction reactor (in kg/s of inlet solids), for the nine scenarios under investigation.

Regarding the make-up material needed to maintain constant conversion rates in the reactors, the computed amounts (plotted in Figure 11) range from 320 to 718 t/yr (equivalent to 56–126 m³/yr). It can be seen in Equation (4) than the required make-up material is affected directly by the material flowing throughout the process. Therefore, the computed flows displayed in Figure 11 are a direct function of the reduction in running hours. Converting the plotted numbers into trucks/yr (assuming a truck payload of 30 tonnes), the resulting values are in the range of 10–24 trucks/yr. Note that a similar flow of oxidized material is required to be purged and sent back to the iron mill.

Make-up requirements (tonnes/yr)
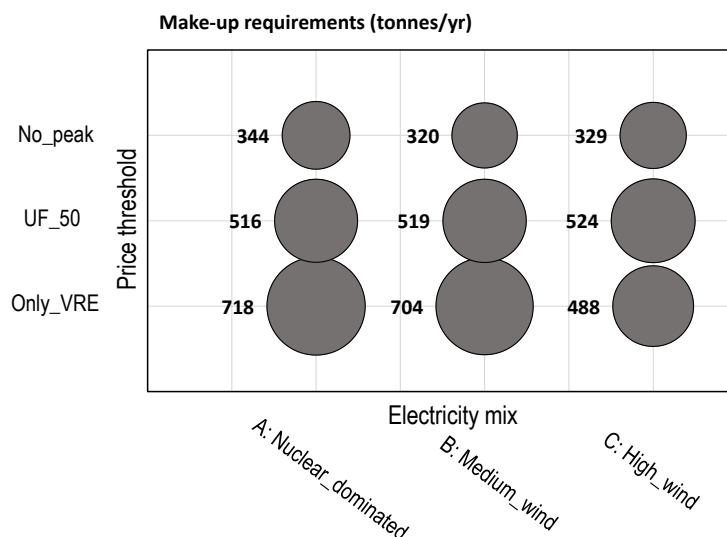
Figure 11. Make-up flow required for each of the nine scenarios under investigation.

6. Discussion

This section discusses (i) the practical implications of the results presented in Section 5, at both the national and plant levels, and (ii) three implementation options that extend beyond the basic process assessed in this work. This discussion highlights the

opportunities and benefits of the scheme in both present and future energy systems and establishes comparisons with other potential options for electricity-based DH.

6.1. Practical Implications

At the national level, given that the installed capacity of Swedish DH plants larger than 20 MW is around 12,500 MW [60], a complete retrofit of the Swedish DH fleet (extrapolating the intermediate scenario, i.e., with the *UF_50* threshold applied, to the *Medium_wind* profile) would require an inventory of around 2.8 Mt of iron material, which is about 0.23% of the Swedish national reserves and approximately 11% of LKAB´s annual production of iron ore (around 27 Mt/yr) [69], so it falls into the feasible national mining capacities. The calculated make-up streams (to cover material losses and deactivation) would amount to about 40 kt/yr for the entire DH fleet in the same scenario, which represents 0.15% of LKAB´s annual production of iron ore. Although a full application of the TCES system investigated in this work will require large amounts of iron ore, it can be concluded that both the Swedish iron reserves and the Swedish iron industry should be able to cover the mass inventories and mass flows required for an iron-based national DH system. This will of course require that a business model be developed such that the metal industry and DH sector discover a mutual economic interest in the concept.

As shown in Figure 8b, the computed energy efficiency of the process for the base case, i.e., with low-temperature electrolyzers, is around 90% (for the preliminary scheme presented here, which does not include any advanced heat integration). Thus, a retrofitted Swedish DH fleet (the current system supplies 50 TWh/yr of heat) would require about 58 TW$_e$h/yr, i.e., a 33% increase in the current level of electricity consumption in Sweden (140 TW$_e$h/yr). This electricity demand for the large-scale implementation of TCES would most likely be met by new wind power capacity (both onshore and offshore). Note that such a high penetration level of renewable electricity in the system would replace the biomass currently consumed for DH production (equivalent to around 15 Mt of CO_2 that could be saved yearly). Because the present solution includes the intermediate transformation of electricity into chemical energy (which can be stored and transported) before being converted into heat, it offers the potential to deliver heat even at times when and places at which the grid is at its maximum capacity. The flexibility offered by the system in allowing for the charging of storage whenever it is convenient removes the need to overdimension the electrical grid transmission and production capacities.

At the plant level, the mass and energy balances confirm the technical ability of the proposed process to satisfy the heat demand that is covered today by DH-generation plants, regardless of the characteristics of the surrounding electricity system (in terms of availability and variability). Furthermore, the required transportation of solid material through the boundaries of a given DH plant that is applying the iron-based scheme is largely reduced compared with the current biomass-based scheme. Thus, in a 100 MW$_{th}$ plant, transportation of solids is decreased from 700 t/day (1240 m³/day) of wood chips (assuming 30% moisture, a heating value of 20 MJ/kg$_{daf}$, and a density of 380 kg$_{dry}$/m³) to 1–2 t/day (0.3–0.7 m³/day) of iron make-up, as depicted in Figure 11 (although the typical distances for biomass transportation are much shorter than those required by the present scheme). For a full assessment of the costs and emissions generated from the transport of solid materials, a more in depth understanding of the quality and reactivity is needed.

A key finding of the present work, displayed in Figures 8 and 9, is that the suggested process involves the addition of a certain nondispatchable DH-generation capacity to the retrofitted plant, in particular for the layout involving low-temperature electrolyzers (the installed capacity is almost double according to the process sizing methodology followed in this work). Thus, as the computed energy and mass balances represent the most conservative process sizing, smaller capacities for the charging side could be achieved if, for example, the oxidation reactor is assumed to operate at the minimum load rather than the maximum load. To illustrate this, a conventional 100 MW$_{th}$ DH peaking plant operating at full load for 6000 h/yr would require an electricity consumption of 0.67 TWh$_e$/r. After

applying the r_{disp} = 44% computed here, 0.264 TWh/yr of heat would be delivered by the oxidation reactor, while 0.336 TWh/yr would be nondispatchable, i.e., produced in the charging section. Note also that the amount of nondispatchable heat generation is reduced in the case with high-temperature electrolyzers (as is the electricity consumption), thereby simplifying the operational scheme because the heat production capabilities are limited to the discharging side (see Figure 7). The higher the dispatchability ratio, the more flexible the operation that the plant offers.

Although detailed equipment sizing is not within the scope of the present work, some rough estimations can be made. The oxidation reactor is meant as a retrofit of a current FB boiler; i.e., its dimensions are previously set. The typical dimensions of a 100 MW$_{th}$ FB furnace are as follows: cross-sectional area in the range of 25–80 m^2 (depending on whether it is of the bubbling or circulating type) and height in the range of 20–30 m. These dimensions ensure that the evaporator membrane walls have a sufficient heat-exchange area for the desired level of heat removal. FB reactors require a certain inventory of solids (30–50 tonnes of sand/ash in the case of a 100 MW$_{th}$ boiler) to achieve adequate thermal mixing and heat transfer rates. The iron residence times and mass flows through the oxidation reactor calculated in this work indicate that the retrofitted unit would require an iron solid inventory of the same order of magnitude. Regarding the reduction reactor to be constructed, it would be adiabatic and thus free of heat-exchange requirements, and its dimensions would reflect the residence time required for the desired conversion and solids throughput.

An additional benefit of the DH process presented in this work, as compared with biomass-based DH plants, is the elimination of emissions (not only CO_2 but also NO_x and SO_x) and alkali-related issues, such as deposition on heat-exchanger surfaces, corrosion, agglomeration, and the handling of the ash output. Indeed, the oxidation of metals would allow for an increased furnace temperature (which thereby increases in the steam data and the thermodynamic process efficiency), as compared with a biomass furnace. Moreover, the cogeneration of electricity (briefly introduced in Section 6.1) is a feasible option.

Rather than dimensioning the storage capacity so that it is capable of covering the longest-possible variations (as typically carried out for other energy storage technologies), the storage is here sized to cover the average variation, characterized by the *ADV* value. ADV is a function of the technology mix for electricity generation and the electricity price threshold for running the charging section. Therefore, periods longer than the *ADV* and during which electricity prices are higher than the threshold cannot be covered by the storage in place. Instead, the scheme presented here offers the possibility to make use of the backup of reduced material at the metal mill (for this case study, located in northern Sweden; see Section 3). To illustrate this, taking the *Medium_wind* profile and the *UF_50* threshold yields one critical period of 470 h (compared with the *ADV* of 64 h) during which the electricity prices are higher than the selected threshold. A full storage unit would provide coverage for the first 64 h, resulting in 406 h of oxidation reactor operation that would need to be supplied by the backup reserve. This translates into 145,000 tonnes (25,600 m^3) of reduced material needing to be freighted over a period of 17 days (by truck, train, or ship, depending on the plant location). Alternative strategies are to add storage capacity or increase the threshold price (i.e., running the reduction section despite the high electricity price). The optimal dimensioning of the storage cannot be elucidated without further detailed economic assessments.

A comparison of the scheme proposed in this work with DH systems based on heat pumps (HP) shows that the main benefit of the iron-based process lies in the dispatchability of heat production. This is highly valuable in terms of both the economic feasibility of the concept (which would otherwise rely on the high price volatility of the electricity) and the management of variations in the electricity system (a benefit that cannot yet be monetized but will likely be decisive in the upcoming energy systems). Heat pumps (with r_{disp} = 0%) need to consume electricity according to the heat demand curve, which at certain times can be extremely costly and exerts stress on the electricity grid. Even though

combining heat pumps with thermal energy storage (HP-TES) would somewhat alleviate these issues by providing a day-scale storage, wind power variations are characterized by longer time scales. Therefore, the resulting r_{disp} of HP-TES systems depends on the *ADV* of the variations to be absorbed, which is not the case for the unlimited time scale offered by the process presented here. Furthermore, the high discharge temperatures in the suggested scheme can deliver dispatchable electricity and industrial heat, making it a more robust solution for future energy systems (see Section 6.1), and it offers the possibility to transport the stored chemical energy in the form of charged (reduced) solid material, assuring high power supply in narrow time periods. On the other hand, HP systems are highly efficient and flexible in extracting low-temperature heat from different sources (air, water, and ground) and are suitable for a wide range of capacities.

The production of hydrogen through electrolysis and its storage for the subsequent production of heat (and power) represent an alternative to the process presented here, given that they would offer similar benefits in terms of absorbing available competitive electricity as a means to increase the penetration of VREs. A proper comparison of these systems is not possible at this point, because the evaluation would be largely dependent on cost variables not included in this work, such as the optimum reactor and storage sizes and costs or the actual price of electricity. Nevertheless, it can be expected that the H2 storage costs would be higher than those associated with the present scheme, given the need for high-pressure containers or processes for chemical binding and given the need for additional safety measures [34]. Furthermore, the possibility to transport the chemically stored energy between different locations, which is one of the key potentials of the process presented here, can be techno-economically challenging for H2-based systems.

6.2. Additional Implementation Options

While the present work focuses on evaluating the basic process scheme linked to the concept, additional implementation options that enhance the technical and economic performances of the base scheme are briefly discussed below. Assessing the suitability of each option is outside the scope of this work and requires a technoeconomic analysis that includes the characteristics of the electricity system and the local heat and hydrogen demands. An overview of the expanded operational modes when factoring in the additional implementation options is given in Section 6.2.4. Schematic process diagrams of the additional implementation options can be found in Figures S1–S3 in the Supplementary Material.

6.2.1. Reduction Hub

To exploit the economy of scale driving the costs of large-scale FB reactors [68,70], the charging sections of several oxidation plants could be merged into a single reduction hub that would consist of a single larger reduction reactor, several electrolyzers, and larger storage units for the solid material (see Figure S1). A major advantage of this option is that the current DH plants would need hardly any retrofitting as the charging section would now be offsite, and the oxidation reactor could be relatively easily adapted from today's FB boiler. In addition, only the hub needs to be connected to the electricity grid. Furthermore, the transport of material to and from the metal mill (according to Figure 4) is minimized as only transportation within the region of influence of the reduction hubs is required, which also means that the efficient transport of large amount of solids needs to be guaranteed.

6.2.2. Cogeneration of Electricity and Industrial Heat

The oxidation of metals with air in FB reactors can occur at temperatures as high as 1100 °C [47]. This feature enables the simultaneous production of electricity and high-temperature heat for, e.g., nearby industrial plants (see Figure S2). This possibility is especially attractive for CHP plants as they already have the power production infrastructure in place and a market for the different services. An additional benefit of this option in future energy systems

is that the added flexibility (derived from the long-duration storage) will be valued much higher than it is today [46], turning the retrofitted DH plants into key players for balancing the electricity grid, not only by absorbing electricity during periods of competitive prices but also by generating electricity during periods of high prices.

6.2.3. On-Demand H$_2$ Production

By splitting the oxidation step into a first stage of oxidation with steam and a second stage with air, the on-demand production of H$_2$ is enabled. Such a configuration, based on the so-called wet metal cycle, is depicted in Figure S3 [71]. Because the metal is reduced during low-electricity-price periods and can be stored indefinitely, the production of H$_2$ in the steam oxidation reactor can adapt to the demand and be decoupled from the electricity prices, without the need for expensive H$_2$ storage. The on-demand production of H$_2$ would be of special interest for heavy transport as the facilities would be distributed throughout the country. Through this alternative process, the energy storage plants would become polygeneration facilities. Note that the use of the air oxidation reactor is mandatory if H$_2$ and dispatchable DH are to be produced simultaneously, because the oxidation with steam has a very low heat of reaction. The need for two oxidation reactors instead of one makes the investment cost of the retrofit much higher than the alternatives described above. However, given the price predictions for green hydrogen [72], this alternative could be financially attractive and is worth considering.

6.2.4. Expanded Operational Modes

The operational map of the plant is expanded as more outputs are considered. Similarly, its utilization and economic performance are expanded. To illustrate this, a scheme for the different operational modes of a polygeneration plant that produces heat, power, and hydrogen on demand is depicted in Figure 12. The different modes are a function of the availability of electricity at competitive prices and the demands for heat and hydrogen. Note that the demand of hydrogen would be defined according to the specific location of the plant as it would be the result of, e.g., the activity of heavy transport or nearby industries. At the same time, the periods during which the electricity price is not competitive represent opportunities for the plant to generate electricity. Provided that there is a demand for hydrogen, it can be produced on the charging side or the discharging side, depending on the electricity price. During periods with competitive electricity prices, the hydrogen can be produced by operating the electrolyzers at higher capacities than those required by the reduction reactor, and during periods of higher electricity prices, the hydrogen can be produced in the steam oxidation reactor. If required, the air oxidation unit can be run in order to profit from the generation of electricity. Note that conventional CHP plants often have the possibility to boost their electricity production by running in condensing mode, which could be exploited during periods of high power demand and low heat demand. Often, the amount of available power at a given time and geographic location is limited by the available grid infrastructure. Thus, periods/locations with such limitations that coincide with demands for hydrogen could be covered by running the steam oxidation.
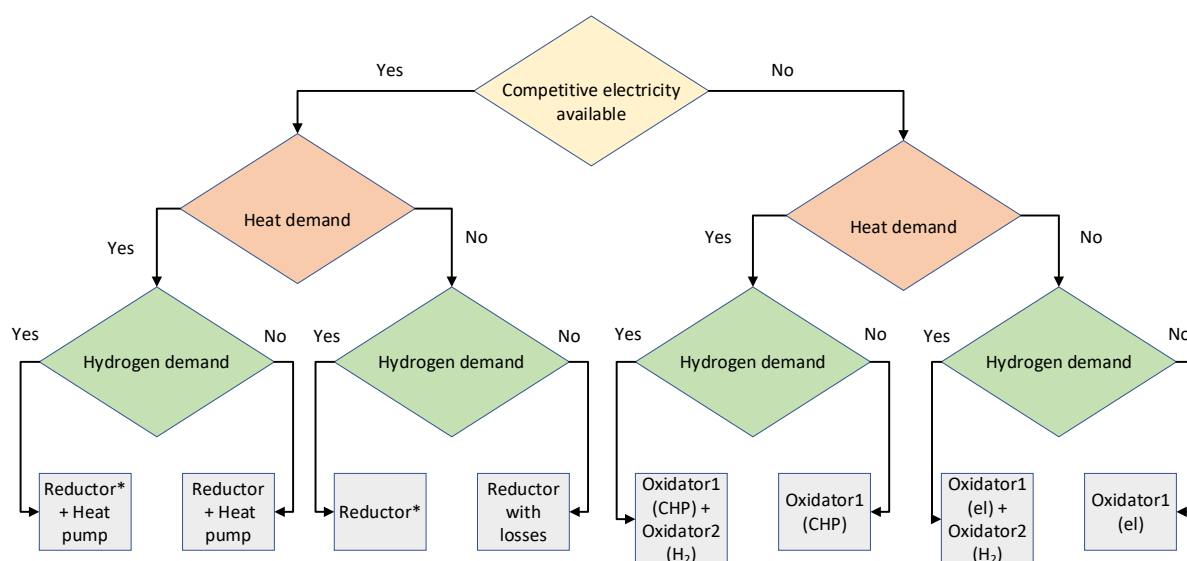
Figure 12. Expanded operational map of a polygeneration plant, based on the suggested process. The operational mode chosen depends on the availability of competitively priced electricity and the demands for heat and hydrogen. Reductor* refers to the reduction section being operated at electrolyzer capacities greater than that required by the reactor.

7. Conclusions

The present work proposed the retrofitting of biomass-fired DH plants into TCES plants on the basis of a high-temperature redox loop, which is able to absorb nondispatchable electricity for storage in the form of reduced metal and can deliver dispatchable, high-temperature heat in a separate stage. A basic layout of the process was proposed, and the technical feasibility of the scheme was assessed on the basis of energy and mass balances computed for a reference Swedish DH plant of typical capacity (i.e., 100 MW$_{th}$). Different scenarios were defined to include differences in the electricity price profiles and characteristic variations of the electricity supply and price, as they relate to the required inventory of stored material and the capacity of the charging section. In addition, two cases (using either low- or high-temperature electrolyzers) were assessed.

The process offers the possibility to generate nondispatchable heat (up to 56% of the total heat production for the case with low-temperature electrolyzers, mainly in the form of recoverable heat losses in the electrolyzers) while the charging section is operated. If the process is instead deployed with high-temperature electrolyzers, the level of electricity consumption is greatly reduced (for the same amount of dispatchable heat produced), as is the generation of nondispatchable heat (only 21% of the total heat produced), thus storing a larger fraction of the absorbed VRE. As for the Swedish case in focus and an intermediate scenario, the inventory of iron oxide required to stock the entire DH network to be converted into the TCES scheme would be around 2.8 Mt, with a make-up flow of 40 kt/yr. This would not have any major impact on the total national metal reserves or iron ore production capacity.

The present work confirmed the potential of the proposed system in future energy systems with different levels of electricity variability as a plausible option for the electrification of DH plants. Further integration into the energy system though the simultaneous generation of electricity and hydrogen is an interesting implementation alternative, as the high temperature of the discharging step provides the opportunity for the generation of electricity by making use of the equipment available in CHP plants. The amount of additional nondispatchable heat that is produced suggests enhanced flexibility to operate the system in several modes, so as to exploit the ability of the system to generate electricity and hydrogen on demand. This opens up the possibility to use the plant for electricity grid-balancing purposes, shifting energy from periods of strong availability (competitive

price) to periods with high demand (higher price) at a seasonal time scale. Nonetheless, assessing the economic feasibility of the process requires refining the process layout and more-detailed calculations that consider the specific boundary conditions of the case to be evaluated.

Nomenclature

ADV	average duration of variations
$F_{red,in}$	solids inflow into the reduction reactor
$F_{oxid,out}$	solids outflow from the oxidation reactor
$H_{2,comb}$	hydrogen required for combustion
$H_{2,red}$	hydrogen required for chemical reduction
$M_{solids,stored}$	inventory of reduced solids stored
M_{system}	total inventory of solids
$N_{lifetime}$	number of cycles within the material lifetime
$\dot{m}_{make-up}$	material make-up flow
r_{disp}	dispatchability ratio
t_{red}	reduction running time
τ_{cycle}	residence time of one cycle
UF	utilization factor

Abbreviations

BECCS	bioenergy with carbon capture and storage
CDR	carbon dioxide removal
CHP	combined heat and power
CLC	chemical looping combustion
DH	district heating
DIR	direction iron reduction
DRI	direct reduced iron
EAF	electric arc furnace
FB	fluidized bed
HP	heat pump
HP-TES	heat pump with thermal energy storage
MSW	municipal solid waste
TCES	thermochemical energy storage
TRL	technology readiness level
VRE	variable renewable electricity

References

1. Nordic Energy Research. *Tracking Nordic Clean Energy Progress 2020—Progress Towards Nordic Carbon Neutrality*; Nordic Energy Research: Oslo, Norway, 2020.
2. IEA. Clean Energy Innovation: Accelerating technology progress for a sustainable future. *Energy Technol. Perspect.* **2020**, 61–89.
3. European Commission, "Accelerating clean energy innovations; clean energy for all Europeans," Brussels, 2016.
4. Nebel, A.; Cantor, J.; Salim, S.; Salih, A.; Patel, D. The Role of Renewable Energies, Storage and Sector-Coupling Technologies in the German Energy Sector under Different CO_2 Emission Restrictions. *Sustainability* **2022**, *14*, 10379. https://doi.org/10.3390/su141610379.
5. Waterson, M.; Baute, E.T.; Giulietti, M. Intermittency and the social role of storage. *Energy Policy* **2022**, *165*, 112947. https://doi.org/10.1016/j.enpol.2022.112947.
6. International Energy Agency. *Technology Roadmap—Energy Storage*; International Energy Agency: Paris, France, 2014.
7. Göransson, L.; Johnsson, F. A comparison of variation management strategies for wind power integration in different electricity system contexts. *Wind. Energy* **2018**, *21*, 837–854. https://doi.org/10.1002/we.2198.
8. Johansson, V.; Göransson, L. Impacts of variation management on cost-optimal investments in wind power and solar photovoltaics. *Renew. Energy Focus* **2020**, *32*, 10–22. https://doi.org/10.1016/j.ref.2019.10.003.
9. Gadd, H.; Werner, S. Thermal energy storage systems for district heating and cooling. In *Advances in Thermal Energy Storage Systems*; Woodhead Publishing: Sawston, UK, 2021; pp. 625–638.
10. Romanchenko, D.; Kensby, J.; Odenberger, M.; Johnsson, F. Thermal energy storage in district heating: Centralised storage vs. storage in thermal inertia of buildings. *Energy Convers. Manag.* **2018**, *162*, 26–38. https://doi.org/10.1016/j.enconman.2018.01.068.
11. Guelpa, E.; Verda, V. Thermal energy storage in district heating and cooling systems: A review. *Appl. Energy* **2019**, *252*, 113474. https://doi.org/10.1016/j.apenergy.2019.113474.
12. Bayon, A.; Bader, R.; Jafarian, M.; Fedunik-Hofman, L.; Sun, Y.; Hinkley, J.; Miller, S.; Lipiński, W. Techno-economic assessment of solid–gas thermochemical energy storage systems for solar thermal power applications. *Energy* **2018**, *149*, 473–484. https://doi.org/10.1016/j.energy.2017.11.084.
13. Prasad, J.S.; Muthukumar, P.; Desai, F.; Basu, D.N.; Rahman, M.M. A critical review of high-temperature reversible thermochemical energy storage systems. *Appl. Energy* **2019**, *254*, 113733. https://doi.org/10.1016/j.apenergy.2019.113733.
14. André, L.; Abanades, S.; Flamant, G. Screening of thermochemical systems based on solid-gas reversible reactions for high temperature solar thermal energy storage. *Renew. Sustain. Energy Rev.* **2016**, *64*, 703–715. https://doi.org/10.1016/j.rser.2016.06.043.
15. Laurie, A.; Abanades, S. Recent Advances in Thermochemical Energy Storage via Solid-Gas Reversible Reactions at High Temperature. *Energies* **2020**, *13*, 5859. https://doi.org/10.3390/en13225859.
16. Li, Z.; Xu, M.; Huai, X.; Huang, C.; Wang, K. Simulation and analysis of thermochemical seasonal solar energy storage for district heating applications in China. *Int. J. Energy Res.* **2020**, *45*, 7093–7107. https://doi.org/10.1002/er.6295.
17. Marie, L.; Landini, S.; Bae, D.; Francia, V.; O'Donovan, T. Advances in thermochemical energy storage and fluidised beds for domestic heat. *J. Energy Storage* **2022**, *53*, 105242. https://doi.org/10.1016/j.est.2022.105242.
18. Debiagi, P.; Rocha, R.; Scholtissek, A.; Janicka, J.; Hasse, C. Iron as a sustainable chemical carrier of renewable energy: Analysis of opportunities and challenges for retrofitting coal-fired power plants. *Renew. Sustain. Energy Rev.* **2022**, *165*, 112579. https://doi.org/10.1016/j.rser.2022.112579.
19. European Commission, Directorate-General for Energy, Kranzl, L.; Fallahnejad, M.; Büchele, R.; Müller, A.; Hummel, M.; Fleiter, T.; Mandel, T.; Bagheri, M.; Deac, G.; et al. *Renewable Space Heating Uunder the Revised Renewable Energy Directive Final Report*; European Commission: Brussels, Belgium, 2021.
20. Osička, J.; Černoch, F. European energy politics after Ukraine: The road ahead. *Energy Res. Soc. Sci.* **2022**, *91*, 102757. https://doi.org/10.1016/j.erss.2022.102757.
21. Rabbi, M.F.; Popp, J.; Máté, D.; Kovács, S. Energy Security and Energy Transition to Achieve Carbon Neutrality. *Energies* **2022**, *15*, 8126. https://doi.org/10.3390/en15218126.
22. Gerard, F.; Opinska, L.G.; Smit, T.; Rademaekers, K.; Braungardt, S.; Monejar Montagud (DTU). *Policy Support for Heating and Cooling Decarbonisation*; European Commission: Brussels, Belgium, 2021.
23. Latõsov, E.; Volkova, A.; Siirde, A.; Kurnitski, J.; Thalfeldt, M. Primary energy factor for district heating networks in European Union member states. *Energy Procedia* **2017**, *116*, 69–77. https://doi.org/10.1016/j.egypro.2017.05.056.
24. Arens, M.; Aydemir, A.; Elsland, R.; Fleiter, T.; Frassine, C.; Herbst, A.; Hirzel, S.; Krail, M.; Ragwitz, M.; Rehfeldt, M.; et al. Mapping and Analyses of the Current and Future (2020–2030) Heating/Cooling Fuel Deployment (Fossil/Renewables); European Commission: Brussels, Belgium, 2016.
25. Vad, B.; Alberg, P.; Connolly, D.; Nielsen, S.; Persson, U. Heat Roadmap Europe 2050. In Proceedings of the IEA CHP/DHC Working Group Joint Strategic Workshop, Aalborg, Denmark, 27–28 May 2014.
26. Lund, H.; Werner, S.; Wiltshire, R.; Svendsen, S.; Thorsen, J.E.; Hvelplund, F.; Mathiesen, B.V. 4th Generation District Heating (4GDH): Integrating smart thermal grids into future sustainable energy systems. *Energy* **2014**, *68*, 1–11. https://doi.org/10.1016/j.energy.2014.02.089.
27. Sorknæs, P. Hybrid energy networks and electrification of district heating under different energy system conditions. *Energy Rep.* **2021**, *7*, 222–236. https://doi.org/10.1016/j.egyr.2021.08.152.

28. Soysal, E.R.; Sneum, D.M.; Skytte, K.; Olsen, O.J.; Sandberg, E. Electric boilers in district heating systems: A comparative study of the Scandinavian market conditions. In Proceedings of the Swedish Association for Energy Economics Conference, Luleå, Sweden, 23–24 August 2016.

29. Sneum, D.M.; Sandberg, E. Economic incentives for flexible district heating in the Nordic countries. *Int. J. Sustain. Energy Plan. Manag.* **2018**, *16*, 27–44.

30. Patronen, J.; Kaura, E.; Torvestad, C. Nordic heating and cooling. Nordic Council of Ministers, Denmark, 2017. https://doi.org/10.6027/tn2017-532.

31. Schweiger, G.; Rantzer, J.; Ericsson, K.; Lauenburg, P. The potential of power-to-heat in Swedish district heating systems. *Energy* **2017**, *137*, 661–669. https://doi.org/10.1016/j.energy.2017.02.075.

32. David, A.; Mathiesen, B.V.; Averfalk, H.; Werner, S.; Lund, H. Heat Roadmap Europe: Large-Scale Electric Heat Pumps in District Heating Systems. *Energies* **2017**, *10*, 578. https://doi.org/10.3390/en10040578.

33. Göransson, L.; Lehtveer, M.; Nyholm, E.; Taljegard, M.; Walter, V. The Benefit of Collaboration in the North European Electricity System Transition—System and Sector Perspectives. *Energies* **2019**, *12*, 4648. https://doi.org/10.3390/en12244648.

34. Hassan, I.; Ramadan, H.S.; Saleh, M.A.; Hissel, D. Hydrogen storage technologies for stationary and mobile applications: Review, analysis and perspectives. *Renew. Sustain. Energy Rev.* **2021**, *149*, 111311. https://doi.org/10.1016/j.rser.2021.111311.

35. Andersson, J.; Grönkvist, S. Large-scale storage of hydrogen. *Int. J. Hydrogen Energy* **2019**, *44*, 11901–11919. https://doi.org/10.1016/j.ijhydene.2019.03.063.

36. Beiron, J.; Göransson, L.; Normann, F.; Johnsson, F. Flexibility provision by combined heat and power plants—An evaluation of benefits from a plant and system perspective. *Energy Convers. Manag. X* **2022**, *16*, 100318. https://doi.org/10.1016/j.ecmx.2022.100318.

37. Gerssen-Gondelach, S.; Saygin, D.; Wicke, B.; Patel, M.; Faaij, A. Competing uses of biomass: Assessment and comparison of the performance of bio-based heat, power, fuels and materials. *Renew. Sustain. Energy Rev.* **2014**, *40*, 964–998. https://doi.org/10.1016/j.rser.2014.07.197.

38. Philibert, C. *Renewable Energy for Industry: Materials and Fuels*; International Energy Agency, Paris, France, 2017.

39. Malico, I.; Pereira, R.N.; Gonçalves, A.C.; Sousa, A.M.O. Current status and future perspectives for energy production from solid biomass in the European industry. *Renew. Sustain. Energy Rev.* **2019**, *112*, 960–977. https://doi.org/10.1016/j.rser.2019.06.022.

40. Searle, S.Y.; Malins, C.J. Waste and residue availability for advanced biofuel production in EU Member States. *Biomass- Bioenergy* **2016**, *89*, 2–10. https://doi.org/10.1016/j.biombioe.2016.01.008.

41. Swedish Energy Agency: State Aid for BECCS," 2022. Available online: http://www.energimyndigheten.se/en/sustainability/carbon-capture-and-storage/state-aid-for-beccs/ (accessed on 9 November 2022).

42. Hanssen, S.V.; Daioglou, V.; Steinmann, Z.J.N.; Doelman, J.C.; Van Vuuren, D.P.; Huijbregts, M.A.J. The climate change mitigation potential of bioenergy with carbon capture and storage. *Nat. Clim. Chang.* **2020**, *10*, 1023–1029. https://doi.org/10.1038/s41558-020-0885-y.

43. Swedish Energy Agency: Statistics, 2022. Available online: https://www.energimyndigheten.se/en/facts-and-figures/statistics/ (accessed on 11 November 2022).

44. Johansson, N. A Faster Pace And Higher Targets in LKAB's Transition Towards a Sustainable Future, Luleå, April 2022. Available online: https://lkab.com/en/press/a-faster-pace-and-higher-targets-in-lkabs-transition-towards-a-sustainable-future/ (accessed on 3 October 2022).

45. Spreitzer, D.; Schenk, J. Iron Ore Reduction by Hydrogen Using a Laboratory Scale Fluidized Bed Reactor: Kinetic Investigation—Experimental Setup and Method for Determination. *Met. Mater. Trans. B* **2019**, *50*, 2471–2484. https://doi.org/10.1007/s11663-019-01650-9.

46. Beiron, J.; Montañés, R.M.; Normann, F.; Johnsson, F. Combined heat and power operational modes for increased product flexibility in a waste incineration plant. *Energy* **2020**, *202*, 117696. https://doi.org/10.1016/j.energy.2020.117696.

47. Adánez, J.; Abad, A.; Mendiara, T.; Gayán, P.; de Diego, L.; García-Labiano, F. Chemical looping combustion of solid fuels. *Prog. Energy Combust. Sci.* **2018**, *65*, 6–66. https://doi.org/10.1016/j.pecs.2017.07.005.

48. Elmquist, S. Operational results of the Circored fine ore direct reduction plant in Trinidad. *Stahl Und Eisen(Ger.)* **2002**, *122*, 59–64.

49. Zhang, H. CFD-DEM Modeling of Gas-Solid Flow and Heat Transfer in A FINEX Melter & Gasifier, Ph.D. Dissertation, UNSW Sydney, Kensington, Australia, 2011.

50. Hillisch, W.; Zirngast, J. Status of Finmet plant operation at BHP in Australia. Steel Times Int., 2001, vol 3 pp. 20–22.

51. Anameric, B.; Kawatra, S.K. Properties and features of direct reduced iron. *Miner. Process. Extr. Met. Rev.* **2007**, *28*, 59–116. https://doi.org/10.1080/08827500600835576.

52. Technology Data. Danish Energy Agency. Available online: https://ens.dk/en/our-services/projections-and-models/technology-data (accessed on 7 November 2022).

53. Liu, T.; Panahi, A. Metal Fuels as Alternative Sources of Energy for Zero Carbon Emission. *IOP Conf. Series: Earth Environ. Sci.* **2021**, *943*, 012016. https://doi.org/10.1088/1755-1315/943/1/012016.

54. Leion, H.; Mattisson, T.; Lyngfelt, A. Use of Ores and Industrial Products As Oxygen Carriers in Chemical-Looping Combustion. *Energy Fuels* **2009**, *23*, 2307–2315. https://doi.org/10.1021/ef8008629.

55. Kobayashi, H.; Hayakawa, A.; Somarathne, K.K.A.; Okafor, E.C. Science and technology of ammonia combustion. *Proc. Combust. Inst.* **2019**, *37*, 109–133. https://doi.org/10.1016/j.proci.2018.09.029.

56. Steinfeld, A.; Kuhn, P.; Reller, A.; Palumbo, R.; Murray, J.; Tamaura, Y. Solar-processed metals as clean energy carriers and water-splitters. *Int. J. Hydrog. Energy* **1998**, *23*, 767–774.

57. Vogl, V.; Åhman, M.; Nilsson, L.J. Assessment of hydrogen direct reduction for fossil-free steelmaking. *J. Clean. Prod.* **2018**, *203*, 736–745. https://doi.org/10.1016/j.jclepro.2018.08.279.

58. Bhaskar, A.; Assadi, M.; Somehsaraei, H.N. Decarbonization of the Iron and Steel Industry with Direct Reduction of Iron Ore with Green Hydrogen. *Energies* **2020**, *13*, 758. https://doi.org/10.3390/en13030758.

59. Pei, M.; Petäjäniemi, M.; Regnell, A.; Wijk, O. Toward a Fossil Free Future with HYBRIT: Development of Iron and Steelmaking Technology in Sweden and Finland. *Metals* **2020**, *10*, 972. https://doi.org/10.3390/met10070972.

60. Kjärstad, J.; Johnsson, F. The European power plant infrastructure—Presentation of the Chalmers energy infrastructure database with applications. *Energy Policy* **2007**, *35*, 3643–3664. https://doi.org/10.1016/j.enpol.2006.12.032.

61. Toktarova, A.; Göransson, L.; Johnsson, F. Design of Clean Steel Production with Hydrogen: Impact of Electricity System Composition. *Energies* **2021**, *14*, 8349. https://doi.org/10.3390/en14248349.

62. Sterner, M.; Stadler, I. *Handbook of Energy Storage*; Springer: Berlin/Heidelberg, Germany, 2019.

63. Böhm, H.; Moser, S.; Puschnigg, S.; Zauner, A. Power-to-hydrogen & district heating: Technology-based and infrastructure-oriented analysis of (future) sector coupling potentials. *Int. J. Hydrogen Energy* **2021**, *46*, 31938–31951. https://doi.org/10.1016/j.ijhydene.2021.06.233.

64. Linderholm, C.; Schmitz, M. Chemical-looping combustion of solid fuels in a 100 kW dual circulating fluidized bed system using iron ore as oxygen carrier. *J. Environ. Chem. Eng.* **2016**, *4*, 1029–1039. https://doi.org/10.1016/j.jece.2016.01.006.

65. Liu, Y.; Zhu, Q.; Zhang, T.; Yan, X.; Duan, R. Analysis of chemical-looping hydrogen production and power generation system driven by solar energy. *Renew. Energy* **2020**, *154*, 863–874. https://doi.org/10.1016/j.renene.2020.02.109.

66. Bahgat, M.; Khedr, M. Reduction kinetics, magnetic behavior and morphological changes during reduction of magnetite single crystal. *Mater. Sci. Eng. B* **2007**, *138*, 251–258. https://doi.org/10.1016/j.mseb.2007.01.029.

67. Patisson, F.; Mirgaux, O. Hydrogen Ironmaking: How it Works. *Metals* **2020**, *10*, 922. https://doi.org/10.3390/met10070922.

68. Castilla, G.M.; Guío-Pérez, D.; Papadokonstantakis, S.; Pallarès, D.; Johnsson, F. Techno-Economic Assessment of Calcium Looping for Thermochemical Energy Storage with CO_2 Capture. *Energies* **2021**, *14*, 3211. https://doi.org/10.3390/en14113211.

69. LKAB. *Annual and Sustainability Report*; LKAB: Luleå, Sweden, 2021.

70. Woods, R.D. *Rules of Thumb in Engineering Practice*; Wiley-VCH: Weinheim, UK, 2007.

71. Rydén, M.; Arjmand, M. Continuous hydrogen production via the steam–iron reaction by chemical looping in a circulating fluidized-bed reactor. *Int. J. Hydrogen Energy* **2012**, *37*, 4843–4854. https://doi.org/10.1016/j.ijhydene.2011.12.037.

72. Glenk, G.; Reichelstein, S. Economics of converting renewable power to hydrogen. *Nat. Energy* **2019**, *4*, 216–222. https://doi.org/10.1038/s41560-019-0326-1.